Macromolecules

Article

pubs.acs.org/Macromolecules

Rationally Controlling the Self-Assembly Behavior of Triarmed POSS−Organic Hybrid Macromolecules: From Giant Surfactants to Macroions

Wei Zhang,[†] Yang Chu,[†] Gaoyan Mu,[†] Seyed Ali Eghtesadi,[†] Yuchu Liu,[†] Zhe Zhou,[†] Xinlin Lu,[†] Marjan Alsadat Kashfipour,[‡] Robert Scott Lillard,[‡] Kan Yue,[§] Tianbo Liu,*[,†] and Stephen Z. D. Cheng*[,†]

[†]Department of Polymer Science, College of Polymer Science and Polymer Engineering, and [‡]Department of Chemical and Biomolecular Engineering, The University of Akron, Akron, Ohio 44325-3909, United States

[§]South China Advanced Institute for Soft Matter Science and Technology, South China University of Technology, Guangzhou 510640, China

Supporting Information

ABSTRACT: Two triarmed organic−inorganic hybrid materials based on carboxylic acid-functionalized polyhedral oligomeric silsesquioxane (APOSS) with/without PS linkers are designed and synthesized (tri-PS-APOSS and tri-APOSS). They can both self-assemble into hollow spherical nanostructures in water/organic mixed solvents, as confirmed by light scattering and TEM techniques, yet they possess completely different mechanisms and driving forces. With the PS linkers, the hybrid forms bilayer vesicles similar to surfactants; while without the PS linkers, the hybrid behaves like hydrophilic macroions and assembles into single-layered, vesicle-like "blackberry"-type structure. Consequently, the trend of the assembly size in response to the change of the solvent polarity is different for the two scenarios. This work shows a simple, universal approach of controlling the mechanism and product of the self-assembly process via minor adjustment of the organic−inorganic hybrid structures.

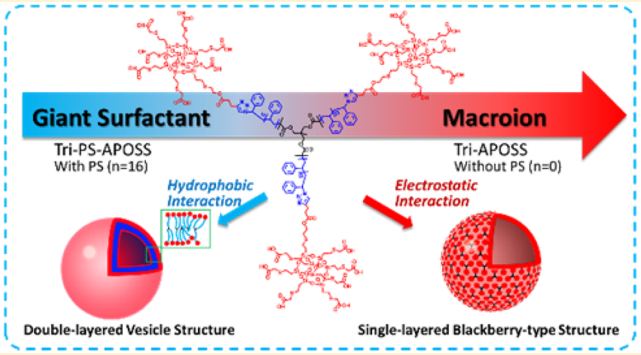

INTRODUCTION

Self-assembly of macromolecules has attracted many researchers due to both fundamental interests and broad applications. These processes are results of the spontaneous inter- and intramolecular interactions of the molecules. The driving forces of the processes are mainly noncovalent interactions, such as hydrogen bonding,[1] electrostatic interactions,[2−4] hydrophobic effect,[5] metal−ligand coordinations,[6,7] $\pi-\pi$ interaction,[8] and other enthalpic interactions in addition to their entropic changes. Tuning and combining different interactions could generate various of interesting morphologies in functional materials.[9−15] On the other hand, tailing macromolecular architecture could also result in polymeric materials with different properties.[16−18] For instance, materials with unique topologies such as dendrimers,[19,20] star polymers,[21,22] miktoarm block copolymers,[23] and many others[23−28] also possess their own unique physical properties.

Giant surfactants are a kind of macromolecule consisting of hydrophilic molecular nanoparticle (MNP) heads and hydrophobic polymeric tails.[29] The MNPs include polyhedral oligomeric silsesquioxane (POSS),[30−33] polyoxometalates (POMs),[34] functionalized fullerenes,[31,35] globular protein,[36] etc., and the tails could be alkyl chains, polystyrene (PS), polycaprolactone, etc.[30,32,35,37,38] The giant molecules fill the gap between small molecular surfactants and amphiphilic diblock copolymers with the ability to form nanosized ordered structures. They have attracted great research interests in the past ten years. Compared to small molecular surfactants, giant surfactants are convenient to be modified and usually contain denser functional groups for multiple interactions and external stimuli.[39−42] On the other hand, they have more precise control on shape-persistent molecular structures compared with diblock copolymers, and therefore their self-assembly structures are relatively uniform to be characterized and formation mechanisms are better to be recognized. For example, we have recently systematically illustrated the effect of number and topology of polar heads on the self-assembled structures of a series of POSS−PS giant surfactants in the bulk and solution.[32,37] Giant surfactants with various architectures have recently been designed and synthesized, such as one head with one tail,[31] multiple heads with one tail,[32,43] and one head with multiple tails,[44] to name a few. However, multiarmed or starlike

Received: May 10, 2017
Revised: June 18, 2017

DOI: 10.1021/acs.macromol.7b00963
Macromolecules XXXX, XXX, XXX−XXX

inorganic–organic hybrid giant surfactants are less discussed.[22,33] Studies on the solution and bulk self-assembly behaviors of giant molecules have shown motivating results that can be related to molecular topological variations. In these systems, the main driving forces for self-assembly are usually hydrogen bonding or hydrophobic interactions.

Macroions refer to a kind of hybrid MNP with certain amount of charges on their surfaces. The most representative macroions are POMs,[45] POSS, metal–organic nanocages, and dendrimers, while other charged MNPs or nanoclusters are also good examples.[42,46,47] The size of macroions (1–10 nm) is in between small molecular ions (at subnanometers) and charged large colloidal particles (at submicrometers to several micrometers). Therefore, they cannot be simply treated as point charges like Na^+ or Cl^- by the Debye–Hückel theory, while they are also quite different from charged colloidal particles, which could be described by the Derjaguin–Landau–Verwey–Overbeek (DLVO theory).[45,48] Previous researches have shown that macroions could self-assembled into a special kind of single layered hollow spherical assemblies known as "blackberry-type" structure in solutions via counterion-mediated interaction.[2,42,49–51]

Considering the distinct driving forces to direct the self-assembly of giant surfactants and macroions, it is intriguing for us to explore the interplay of hydrophobic and electrostatic interactions in these hybrid materials with similar architectures. For this purpose, we here reported the design and synthesis of two triarmed macromolecules tri-PS-APOSS and tri-APOSS with or without hydrophobic PS spacer between the core and hydrophilic functionalized POSS. Their self-assembly behaviors in solution clearly demonstrate that tuning the overall hydrophobicity of hybrid molecules can alter the mechanisms of nanostructure formation from giant surfactants to macroions, which are controlled by different driving forces.

■ EXPERIMENTAL SECTION

Materials. Octavinyl POSS was used as received from Hybrid Plastics. Inhibitor was removed from styrene before polymerization by filtering through a silica gel column. All the other chemicals and solvents were used as received from Sigma-Aldrich, Acros Organic, or Fisher Scientific.

Characterization. ^{1}H and ^{13}C NMR experiments were measured on a Varian Mercury 500 NMR spectrometer with reference to the residual solvent peaks of $CDCl_3$ at δ 7.27 and 77.00 ppm or DMSO at 2.50 and 39.52 ppm, respectively. Infrared spectra were measured on an Excalibur Series FT-IR spectrometer (DIGILAB, Randolph, MA) by drop-casting sample films on a KBr disk from THF solution (~10 mg/mL). Gel permeation chromatography (GPC) were measured in THF at 35 °C on Tosoh EcoSEC instrument with three columns [TSKgel SuperH3000 × 2, TSKgel SuperH5000] with a GuardColumn (TSKgel SuperH1000-4000) and a UV detector. The flow rate was 0.35 mL/min. Matrix-assisted laser desorption/ionization time-of-flight (MALDI-TOF) mass spectra were measured on a Bruker Ultra flex III TOF/TOF mass spectrometer under linear mode using salt and DCTB matrix.

Transmission electron microscopic (TEM) images were collected on a JEOL-1230 TEM with an accelerating voltage of 120 kV and a CCD camera.

Sample Preparation for Light Scattering. For a typical sample preparation of tri-PS-APOSS with the concentration of 0.20 mg/mL, 1.0 mg sample was dissolved in 5.0 mL of THF and sonicated for 30 min. A certain amount of ultrapure water (0.05 μs/cm from a Millipore filtration system, pH 6–7) was titrated drop by drop into the solution at the rate of 50 μL/h. Water was stopped to be added until the water content reached 10% v/v.

For tri-APOSS with the concentration of 0.2 mg/mL, each of 1.0 mg sample was dissolved in 1.5, 2.0, 2.5, and 3.0 mL of acetone and sonicated for 30 min. After completely dissolving in acetone, 4.5, 3.0, 2.5, and 2.0 mL of water were added one shot into each solution. After mixing with vibration for 1 min, 70, 60, 50, and 40% v/v water/acetone tri-APOSS sample solutions were prepared.

Light scattering experiments were performed on a commercial Brookhaven laser scattering spectrometer that was equipped with a 637 nm laser. For static light scattering, the angle from 30° to 120° with an interval of 3° was applied. The radius of gyration (R_g) was directly calculated by the Rayleigh–Gans–Debye equation from the software. For dynamic light scattering, an intensity–intensity BI-9000AT correlator was used to get the correlation function based on the particle movement. Three repeating measurements for each sample, and each measurement takes 3 min to get an average scattering intensity and time correction function. All of the measurements are done in 90°, 75°, 60°, and 45° scattering angles to extrapolate the R_h at 0°.

Synthetic Procedures. *VPOSS-S-OH (1).* VPOSS (30 g, 47.3 mmol) was dissolved in tetrahydrofuran (THF, 300 mL). 2-Mercaptoethanol (3.35 g, 43.0 mmol) and photoinitiator 2-hydroxy-4′-(2-hydroxyethoxy)-2-methylpropiophenone (Irgacure 2959, 0.193 g, 0.86 mmol) were added. The solution was irradiated by the 365 nm UV light for 15 min. The crude product was purified by silica gel chromatography (CH_2Cl_2:hexane 1:2) to afford the product as a white powder (7.13 g, 10.0 mmol) in 23% yield. ^{1}H NMR ($CDCl_3$, 500 MHz, ppm, δ): 6.18–5.87 (m, 21H), 3.72 (t, 2H), 2.75 (t, 2H), 2.70–2.61 (m, 2H), 2.00 (br, 1H), 1.11–1.05 (m, 2H). ^{13}C NMR ($CDCl_3$, 125 MHz, ppm, δ): 137.00, 128.58, 60.03, 35.04, 25.56, 13.23.

VPOSS-S-Alkyne (2). VPOSS-S-OH (985 mg, 1.39 mmol, 1 equiv), 4-pentynoic acid (207 mg, 2.11 mmol), and catalyst 4-(dimethylamino)pyridine (DMAP, 17 mg, 0.14 mmol) were dissolved in anhydride CH_2Cl_2 (50 mL). *N,N′*-Diisopropylcarbodiimide (DIPC, 350 mg, 2.78 mmol) was added slowly at 0 °C. The mixture was stirred overnight. The insoluble part was removed by filtration. The solution was concentrated and purified by chromatography on silica gel (CH_2Cl_2:hexane 1:1) to afford VPOSS-alkyne (641 mg, 0.81 mmol) in 58% yield as a white powder. ^{1}H NMR ($CDCl_3$, 500 MHz, ppm, δ): 6.19–5.87 (m, 21H), 4.26 (t, 2H), 2.77 (t, 2H), 2.71–2.68 (m, 2H), 2.59–2.49 (m, 4H), 1.98 (t, 1H), 1.11–1.03 (m, 2H). ^{13}C NMR ($CDCl_3$, 125 MHz, ppm, δ): 171.44, 137.02, 128.64, 128.61, 128.59, 82.32, 69.07, 63.66, 33.25, 30.17, 26.36, 14.33, 13.17.

Tri-Br (3). 1,1,1-Tris(hydroxymethyl)ethane (1.0 g, 8.33 mmol) and Et_3N (5.0 g, 50 mmol) were added in anhydrous THF (50 mL) in a 250 mL flask. Then 2-bromoisobutyryl bromide (11.5 g, 50 mmol) in 20 mL of anhydrous THF was added dropwise into the flask at 0 °C. The reaction mixture was stirred overnight before the insoluble part was filtered. The filtration was concentrated by rotary evaporation, and the residue was purified by a silica gel column (EA:hexane 1:20). The product was obtained as a light yellow sticky solid (3.5 g, 6.17 mmol) in 74% yield. ^{1}H NMR ($CDCl_3$, 500 MHz, ppm, δ): 4.16 (s, 6H), 1.93 (s, 18H), 1.16 (s, 3H). ^{13}C NMR ($CDCl_3$, 125 MHz, ppm, δ): 171.13, 66.62, 55.37, 39.68, 30.70, 17.05.

Tri-PS-Br (4). Styrene (12.0 g, 115 mmol), initiator (tri-Br) (109 mg, 0.19 mmol), and CuBr (83 mg, 0.58 mmol) in toluene (12 g) was added into a 100 mL Schlenk flask. After degassed by three freeze–pump–thaw cycles, *N,N,N′,N″,N″*-pentamethyldiethylenetriamine (PMDETA, 111 mg, 0.58 mmol) was added quickly under a nitrogen atmosphere. The reaction mixture was put in 110 °C oil bath under vigorous stir for 50 min before being quenched in ice–water bath. Then, a short silica gel was used to remove the copper complex. The collected solution was concentrated and precipitated into methanol. The polymer was collected by filtration as a white solid (730 mg, 6% yield). ^{1}H NMR ($CDCl_3$, 500 MHz, ppm, δ): 7.40–6.30 (m, 255H), 4.60–4.38 (m, 6H), 3.30–3.15 (m, 6H), 2.60–1.20 (m, 153H), 1.02–0.80 (m, 18H), 0.51 (m, 3H). GPC: M_n = 4.5 kg mol^{-1}, PDI = 1.10.

Tri-PS-N$_3$ (5). Tri-PS-Br (680 mg, 0.15 mmol) and NaN_3 (285 mg, 4.38 mmol) were added in a 50 mL flask. Dimethylformamide (DMF, 30 mL) was added as solvent. After stirred for 24 h, the mixture was poured into 300 mL of CH_2Cl_2 and then was washed by water (200

DOI: 10.1021/acs.macromol.7b00963
Macromolecules XXXX, XXX, XXX–XXX

Scheme 1. Synthesis of Tri-PS-APOSS[a]

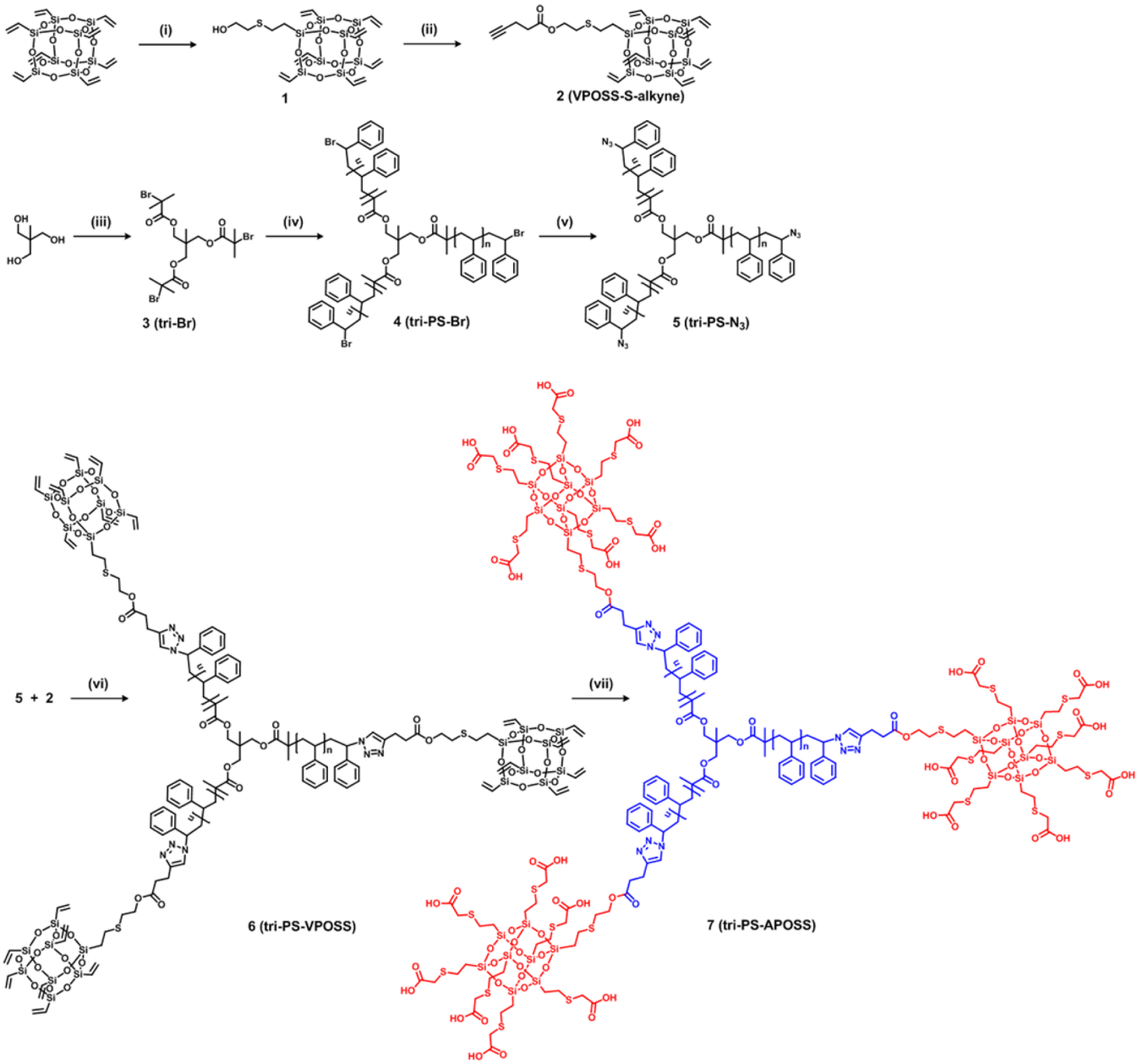

[a]Reaction conditions: (i) 2-mercaptoethanol, Irgacure 2959, THF, 365 nm UV; (ii) 4-pentynoic acid, DIPC, DMAP, CH_2Cl_2; (iii) 2-bromoisobutyryl bromide, Et_3N, THF; (iv) styrene, CuBr, PMDETA, toluene; (v) NaN_3, DMF; (vi) CuBr, PMDETA, toluene; (v) NaN_3, DMF; (vii) thioglycolic acid, Irgacure 2959, THF, 365 nm UV.

mL × 3). After being dried by anhydrous Na_2SO_4, the organic layer was concentrated followed by precipitation into methanol. The product was collect by filtration as a white solid (583 mg, 88%). ^{1}H NMR ($CDCl_3$, 500 MHz, ppm, δ): 7.40−6.30 (m, 255H), 4.05−3.85 (m, 6H), 3.27−3.15 (m, 6H), 2.40−1.20 (m, 153H), 1.01−0.80 (m, 18H), 0.51 (m, 3H). GPC: M_n = 4.5 kg mol^{-1}, PDI = 1.10.

*Tri-PS-VPOSS (**6**).* VPOSS-alkyne (150 mg, 0.19 mmol), tri-PS-N_3 (M_n = 4.5 kg mol^{-1}, 263 mg, 0.058 mmol), and CuBr (1 mg, 0.006 mmol) in 20 mL of toluene was added into a 100 mL Schlenk flask. After three times freeze−pump−thaw, 3 drops of PMDETA was added under a nitrogen atmosphere. The reaction was then conducted under ambient temperature for 24 h. A flash silica gel column was used (CH_2Cl_2 to THF) to give the crude product, which was precipitated into methanol and collected by filtration to afford the product as a white powder (390 mg, 90% yield). ^{1}H NMR ($CDCl_3$, 500 MHz, ppm, δ): 7.40−6.35 (m, 255H), 6.20−5.87 (m, 63H), 5.16−4.92 (m, 6H), 4.24−4.14 (m, 6H), 3.30−3.15 (m, 6H), 3.10−2.56 (m, 24H), 2.40−1.20 (153H), 1.09 (m, 6H), 1.03−0.79 (m, 18H), 0.51 (m, 3H). GPC: M_n = 6.6 kg mol^{-1}, PDI = 1.10.

*Tri-PS-APOSS (**7**).* Tri-PS-VPOSS (100 mg, 0.016 mmol), thioglycolic acid (180 mg, 1.68 mmol), and a small amount of Irgacure 2959 were added in 3 mL THF. The mixture was illuminated under 365 nm UV for 10 min, followed by precipitation into water. The product was collected by filtration as a white solid (120 mg, 88%). ^{1}H NMR ($CDCl_3$, 500 MHz, ppm, δ): 10.95 (br, 21H), 7.40−6.35 (m, 155H), 5.14−4.90 (m, 6H), 4.17 (m, 6H), 3.75−3.50 (m, 6H), 3.35−3.15 (m, 42H), 3.07−2.53 (m, 66H), 2.40−1.20 (m, 153H), 1.15−0.80 (m, 66H), 0.50 (m, 3H). GPC: M_n = 7.2 kg mol^{-1}, PDI = 1.10.

*Tri-N_3 (**8**).* The procedure was similar to that of preparation of tri-PS-N_3. Pure product was obtained by silica gel chromatography (CH_2Cl_2) as a colorless viscous liquid in 85% yield. ^{1}H NMR ($CDCl_3$, 500 MHz, ppm, δ): 4.14 (s, 6H), 1.47 (s, 18H), 1.14 (s, 3H). ^{13}C

DOI: 10.1021/acs.macromol.7b00963
Macromolecules XXXX, XXX, XXX−XXX

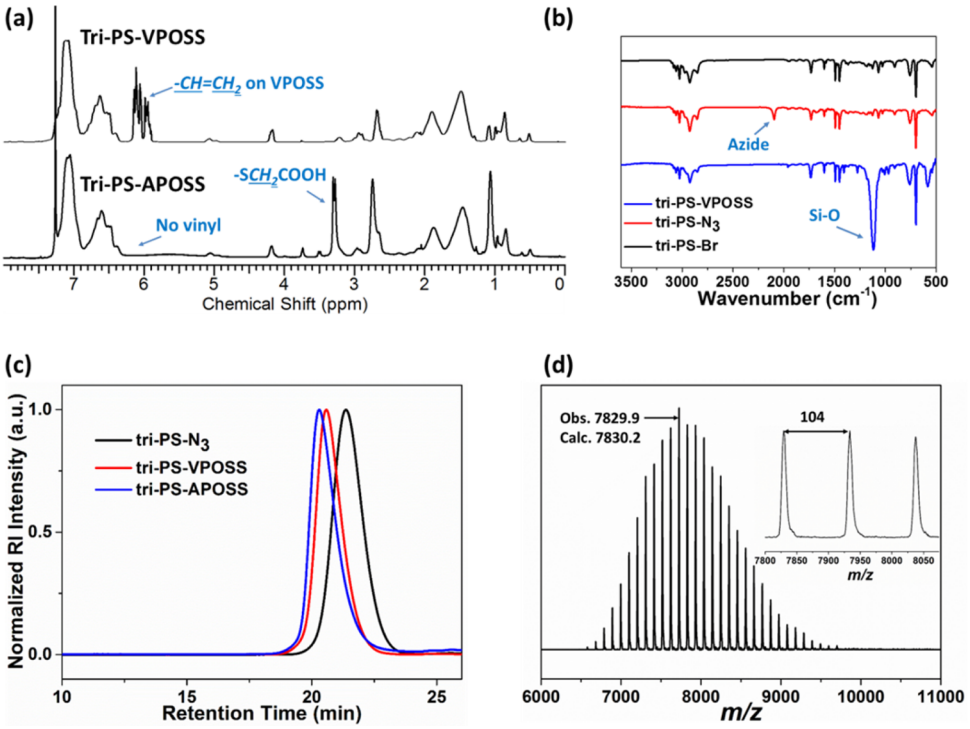

Figure 1. (a) ^{1}H NMR spectra of tri-PS-VPOSS and tri-PS-APOSS. (b) FT-IR spectra of tri-PS-Br, tri-PS-N_3, and tri-PS-VPOSS. (c) GPC traces of tri-PS-N_3, tri-PS-VPOSS, and tri-PS-APOSS. (d) MALDI-TOF spectrum of tri-PS-VPOSS, in which the inset is zoomed.

Scheme 2. Synthesis of Tri-APOSS[a]

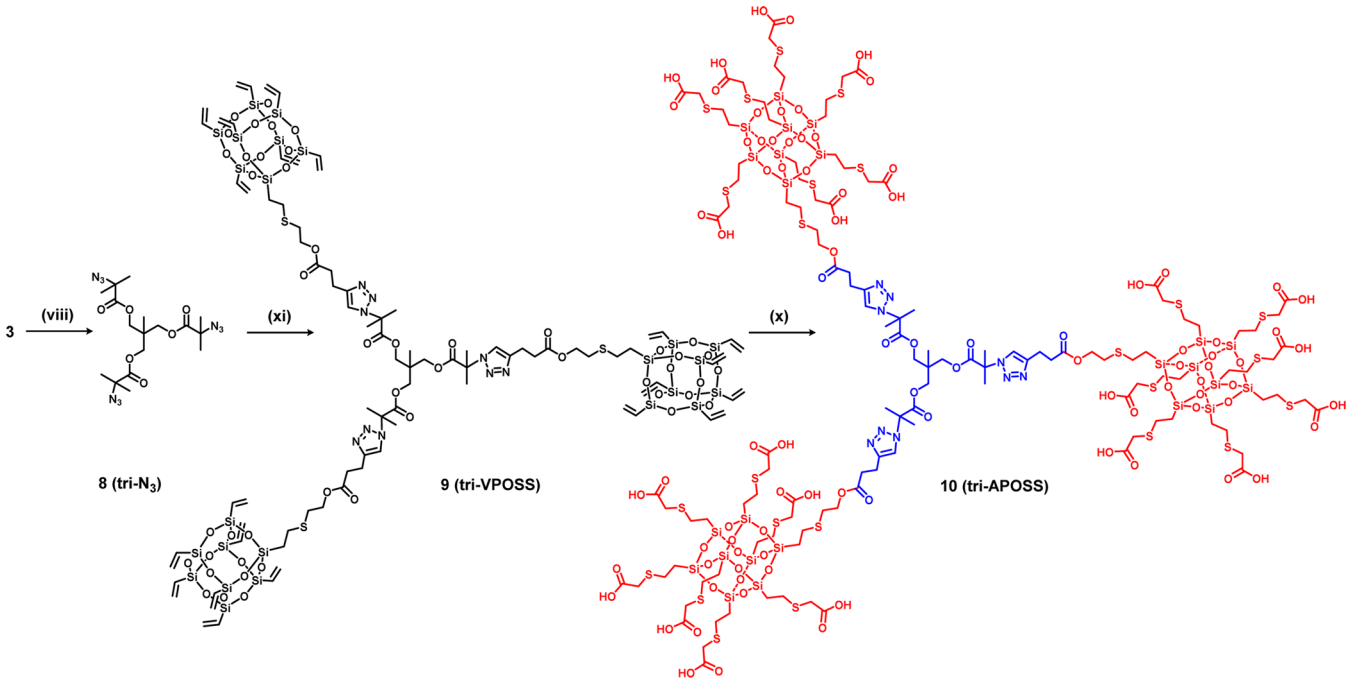

[a]Reaction conditions: (viii) NaN_3, DMF; (xi) VPOSS-S-alkyne, CuBr, PMDETA, toluene; (x) thioglycolic acid, Irgacure 2959, THF, 365 nm UV.

NMR ($CDCl_3$, 125 MHz, ppm, δ): 172.26, 66.38, 63.19, 39.05, 24.35, 17.14.

*Tri-VPOSS (**9**).* The procedure was similar to that of preparation of tri-PS-VPOSS using Cu-catalyzed "click" reaction. The product was obtained as a white solid in 91% yield. ^{1}H NMR ($CDCl_3$, 500 MHz, ppm, δ): 7.53 (s, 3H), 6.12−5.87 (m, 63H), 4.21 (t, 6H), 3.60 (s, 6H), 3.03 (t, 6H), 2.76−2.72 (m, 12 H), 2.69−2.64 (m, 6H), 1.89 (s, 18 H), 1.08−1.05 (m, 6H), 0.63 (s, 3H). ^{13}C NMR ($CDCl_3$, 125 MHz, ppm, δ): 172.39, 170.64, 145.94, 137.02, 136.98, 128.57, 128.62, 128.59, 128.57, 119.82, 65.85, 64.05, 63.27, 38.71, 33.38, 30.18, 26.27, 25.50, 24.35, 20.89, 16.54, 13.16.

*Tri-APOSS (**10**).* The procedure was similar as that of preparation of tri-PS-APOSS. The product was obtained as a white solid in 60% yield. ^{1}H NMR (DMSO, 500 MHz, ppm, δ): 8.03 (s, 3H), 4.15 (t, 6H), 3.63 (m, 6H), 3.24−3.18 (m, 42H), 2.88 (t, 6H), 2.74 (t, 6H), 2.68−2.60 (m, 54H), 1.89−1.80 (m, 21H), 1.04−0.95 (m, 48H), 0.58 (s, 3H).

DOI: 10.1021/acs.macromol.7b00963
Macromolecules XXXX, XXX, XXX−XXX

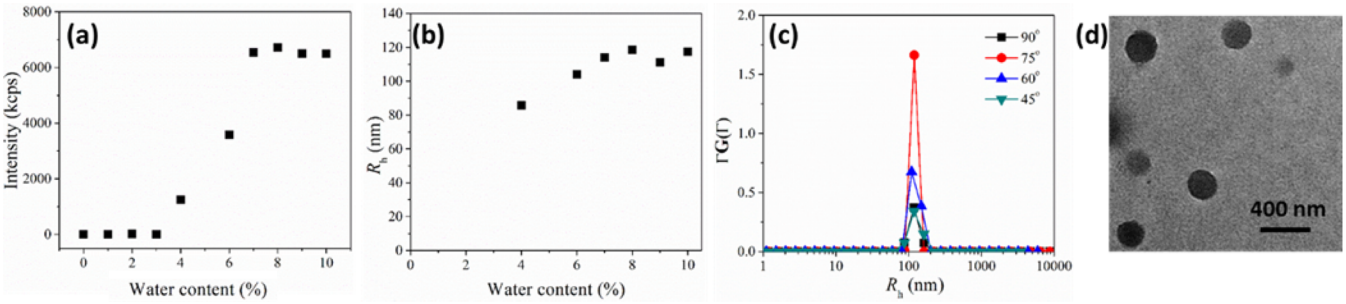

Figure 2. (a) Scattering intensity and (b) R_h values of tri-PS-APOSS in H_2O/THF mixed solvent at 90° scattering angle with different water content. (c) R_h distributions of tri-PS-APOSS in 10% v/v H_2O/THF mixed solvent at different scattering angles and (d) the corresponding TEM image.

^{13}C NMR (DMSO, 125 MHz, ppm, δ): 172.41, 172.32, 172.18, 172.11, 171.02, 145.57, 121.33, 66.13, 64.13, 63.26, 49.05, 33.88, 33.78, 33.31, 29.89, 26.18, 26.14, 25.67, 25.34, 21.49, 21.01, 16.25, 12.90, 12.45.

■ RESULTS AND DISCUSSION

Synthesis. A divergent strategy is utilized to prepare the triarmed giant surfactants (Scheme 1). A small molecular initiator core with three initiation sites was applied to polymerize styrene using atom-transfer radical polymerization (ATRP). The resulting triarmed star PS showed a narrow molecular weight distribution with an apparent number-average molecular weight of 4.5 kg mol^{-1} (Table S1). Then, azide groups were installed to the chain ends to afford tri-PS-N_3, which is ready for in the copper(I)-catalyzed alkyne−azide cycloaddition (CuAAC) "click" reaction. After this substitution, the signal of chain end protons shifted from ∼4.5 ppm (−C$\underline{H}$−Br) to ∼3.9 ppm (−C$\underline{H}$−N_3) in ^{1}H NMR spectra (Figures S7 and S8). A slightly excess amount of VPOSS-alkyne (1.1 equiv per −N_3) was reacted with tri-PS-N_3 under a typical condition for CuAAC "click" reactions to attach the precursor VPOSS moieties. After the "click" reaction, complete disappearance of the azide group at 2100 cm^{-1} in FT-IR spectra was observed, as shown in Figure 1b. The narrow-dispersed peak of GPC curve (Figure 1c) shifted to smaller retention volumes with an apparent molecular weight of 6.6 kg mol^{-1} (Table S1), suggesting no side reaction. Representative peaks of vinyl groups on VPOSS cages (6.2−5.9 ppm) were clearly observed in ^{1}H NMR spectrum as well (Figure 1a). The molecular weight of tri-PS-VPOSS is estimated to be 7.8 kg mol^{-1} by calculation based on the integration of VPOSS (6.2−5.9 ppm, 63H) and PS parts (7.4−6.3 ppm), indicating roughly 16 styrene repeat units (n) in each arm. This result matched well with the single distributed MALDI-TOF (matrix-assisted laser desorption/ionization time-of-flight) mass spectrum as shown in Figure 1d. The strongest peak of $[M + Ag]^+$ in Figure 1d located at m/z = 7829.9 is well consistent with the theoretical molecular weight 7830.2 (n = 16). The slightly small molecular weights for the polymers measured by GPC (7.2 kg mol^{-1}, Table S1) is probably due to the smaller hydrodynamic radius of the polymers with star-shaped geometry compared with their linear counterparts. Lastly, the hydrophilic carboxylic acid groups were introduced to the POSS cages by photoinitiated thiol−ene reaction of tri-PS-VPOSS and thioglycolic acid under the illumination of 365 nm UV light.[32,S2] After the reaction, the peaks of vinyl (6.2−5.9 ppm) completely disappeared, and correspondingly, signals from −$\underline{CH_2}$COOH (∼3.2 ppm) and −$\underline{CH_2}$S− (∼2.7 ppm) emerged in the ^{1}H NMR spectrum of tri-PS-APOSS.

The triarmed tri-APOSS without hydrophobic PS moieties was also synthesized using the same method for comparison in the self-assemble process (Scheme 2). The detailed chemical structure characterizations are listed in the Supporting Information.

Self-Assembly of Tri-PS-APOSS into Bilayer Vesicle Structures. Tri-PS-APOSS is soluble in most organic solvents (e.g., THF, acetone, 1,4-dioxane, DMF) but insoluble in water. The solution of tri-PS-APOSS in THF (0.2 mg/mL) shows very weak scattering intensity increase in static light scattering (SLS) measurements within several weeks, indicating that no supramolecular structures are formed. To induce the self-assembly, water is slowly added to the solution (50 μL/h). Scattering intensity starts to increase at the water content of roughly 4% v/v, suggesting that the giant surfactants start to self-assemble. The intensity keeps increasing with further addition of water until the water content reaches ∼7% v/v, after which the intensity remains constant even more water is added (Figure 2a). It is suggested that the assemblies are stabilized at this stage. Based on the COUTIN analysis of DLS measurements, the change of the average R_h of the assemblies at different water contents is shown in Figure 2b. R_h at 90° scattering angle is stabilized around 115 nm even more water is added. It can also be seen by the right shift of the R_h distribution peak in Figure S16. The narrowly distributed peaks indicate close to monodispersed assemblies. The R_h value does not show obvious angular dependence (Figure 2c), suggesting that the self-assemblies are structurally anisotropic, which is further confirmed by the transmission electron microscopic (TEM) images (Figure 2d, spherical structures). By extrapolating the R_h values to 0° scattering angle, the R_h at 0° can be obtained as 119 nm (Table S2). Comparing it to the radius of gyration (R_g = 119 nm, Table S2), the ratio of R_g/R_h = 1, indicating that the mass of such spherical assemblies is distributed on the surface as hollow spheres.

A bilayer vesicle structure is inferred for this hollow, spherical assembled structure due to the amphiphilic nature of the molecules, which makes tri-PS-APOSS a giant surfactant. As more and more water is added into THF, the size of the self-assemblies starts to increase. The increment of the water amount in THF leads to an increase of solvent polarity, and it makes the hydrophobic PS linkers stay closer to each other to avoid contacting with the solvent. The closer packing of PS linkers results in the increase of the energy cost for bending, thus the decrease of the vesicular curvature and consequently the increase of the assembled size.

The bilayer vesicle structures are further confirmed by atomic force microscopy (AFM). The thickness measured by AFM is ∼25 nm (Figure 3b). The total length of an APOSS group, a PS

DOI: 10.1021/acs.macromol.7b00963
Macromolecules XXXX, XXX, XXX−XXX

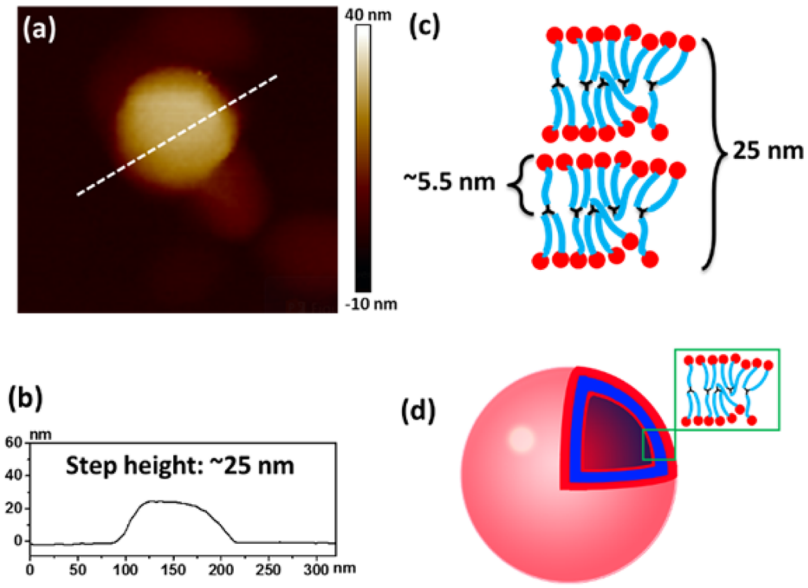

Figure 3. (a) AFM images and (b) height profile of collapsed assemblies after solvent evaporation of tri-PS-APOSS assemblies solution. (c) Schematic illustration of collapsed double-layer assembly model. (d) The model of vesicle structure formed by tri-PS-APOSS.

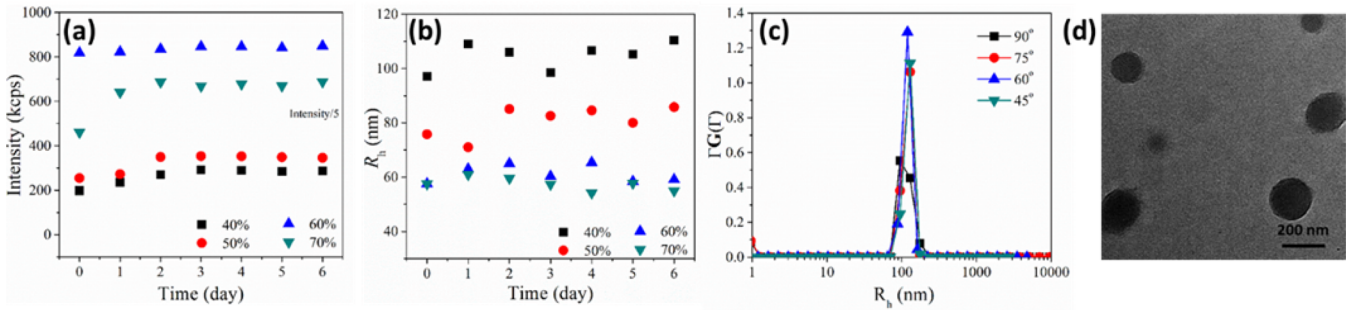

Figure 4. (a) Light scattering intensity and (b) R_h values of tri-APOSS in 40, 50, 60, and 70% v/v H_2O/acetone mixed solvents at 90° scattering angle, (c) R_h distributions of tri-APOSS in 40% v/v H_2O/acetone mixed solvents at different angles, and (d) the corresponding TEM image.

linker with 16 repeating units ($R_0 = (N_{PS}/6.92)^{1/2}b$,[35] where N_{PS} is the degree of polymerization (16 here) and b is the Kuhn length of PS (1.8 nm)), and a short organic linker is estimated to be 5.5 nm. Therefore, the measured thickness of 25 nm is about the stacking of four layers of PS and APOSS. The collapsed four layers measured by AFM indicates a bilayer vesicle structure in solution, as shown in Figure 3c. Based on all the evidence above, a packing model of tri-PS-APOSS is proposed in Figure 3d. The three PS linkers in one molecule can randomly fold to one side or two sides (not distinguishable) and stay between APOSS head groups. Therefore, the main driving force of the self-assembled bilayer vesicle structures is the hydrophobic interaction of the long PS linkers.

Self-Assembly of Tri-APOSS into Single-Layer Blackberry-Type Structures. Tri-APOSS is very soluble in acetone but insoluble in water. No obvious intensity increase in SLS is observed within several weeks in the acetone solution of tri-APOSS. Different amounts of water are added to acetone to tune the solvent polarity. The scattering intensities of the samples with water contents ranging from 40 to 70% v/v start to increase after 1 day (Figure 4a), indicating a lag phase before the self-assembly, which is similar to the situation of "blackberry" structure formation of macroions.[50] The intensity becomes stabilized after 2 days, suggesting that the equilibrium of the system is reached. The sizes of the assemblies of tri-APOSS in different solvents do not have a significant change within a week (Figure 4b), and the R_h distributions are angular independent (in Figure 4c and Figure S18). The ratios of R_g/R_h are all close to 1, suggesting that the spherical assemblies are also hollow. TEM images further confirm the hollow, spherical structure of the assemblies (Figure 4d).

Because of the lack of hydrophobic interaction in the molecule as well as the partially deprotonation of carboxylic acid groups on the POSS, tri-APOSS is rather a macroion than a giant surfactant. The hollow spherical structure is thus expected to be the charge regulated single layer "blackberry"-type structure as reported before.[2,42,50] This hypothesis is supported by the experimental observations. First, an increase of water amount increases the solvent polarity rises the deportation of APOSS head groups. More negative charges on APOSS cages result in increment of electrostatic repulsion between the neighbor APOSS groups. This increment of charges cause less molecules to associate with each other and weaken the bending modulus of the assembled structure. Therefore, the curvature of the self-assembled spheres increases, and the assembly size decreases.[53] Furthermore, a linear relationship is observed when the R_h of tri-APOSS assemblies in different solvents is plotted versus the reverse dielectric constant of the solvent ($1/\varepsilon$) (Figure 5e), which is a major characteristics of charge-regulated self-assembly.[54] The

DOI: 10.1021/acs.macromol.7b00963
Macromolecules XXXX, XXX, XXX−XXX

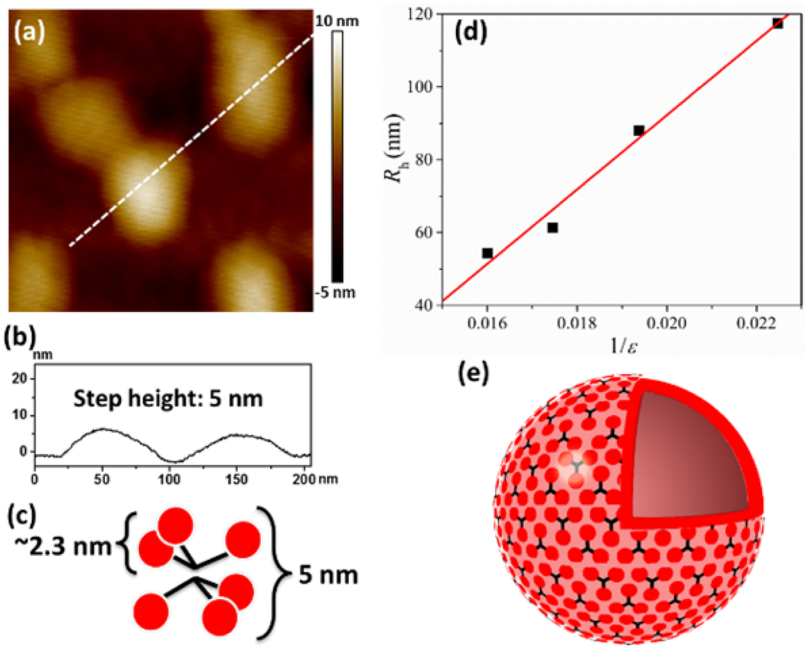

Figure 5. (a) AFM images and (b) height profile of collapsed assemblies after solvent evaporation of tri-PS-APOSS assemblies' solution. (c) Schematic illustration of collapsed single-layer assembly model. (d) Plot of the average hydrodynamic radius (R_h) of tri-APOSS at 90° scattering angle versus the reverse dielectric constant ($1/\varepsilon$) of H_2O/acetone mixed solvents. (e) The model of blackberry structure formed by tri-APOSS.

height profile for the AFM image of the self-assemblies from 70% v/v H_2O/acetone mixed solvent (Figure 5a,b) shows that the thickness the assemblies are ∼5 nm, significantly smaller than the assemblies of tri-PS-APOSS. Considering the thickness of one single tri-APOSS is around 2.3 nm, the total thickness of 5 nm contains two layers of tri-APOSS in the self-assembled structures (Figure 5c), indicating the self-assembled structure in solution is a single layer hollow spherical structure. Based on all the evidence, the hollow spherical structure is the "blackberry"-type structure (Figure 5e),[2,42,50] driven by the counterion-mediated electrostatic interaction. The hydrophobic interaction is negligible in this sample because the hydrophobic organic linker is very short.

Comparing the Self-Assembly Behavior of Tri-PS-APOSS and Tri-APOSS. Both tri-PS-APOSS and tri-APOSS can form hollow spherical structures in the water/organic mixed solvents. However, for tri-PS-APOSS, the hydrophobic PS linkers are long and flexible so that hydrophobic interaction is important, leading to the bilayer vesicle structures. The size of the vesicle slightly increases as more solvent polarity increases. While for tri-APOSS, the hydrophobic interaction is no longer a dominating driving force due to the lack of PS linkers. The short organic linkers can be effectively covered by the three large APOSS heads in each molecule. The protons in the carboxylic acid groups are easily released in the water/acetone mixed solvents, which makes the APOSS heads negatively charged and become strongly hydrophilic. In this case, the electrostatic interaction becomes the main driving force for the self-assembly. The trend of the solvent-responsive size change is completely opposite to the case of tri-PS-APOSS, demonstrating two completely different self-assembly mechanisms.

■ CONCLUSION

Two specially designed triarmed organic−inorganic hybrids are synthesized in this work. Both can self-assemble into hollow spherical structures in the mixture of organic solvent and water but demonstrate different assembly structures and mechanisms. The tri-PS-APOSS molecules behave like giant surfactants by forming double-layered vesicles driven by hydrophobic interaction, while tri-APOSS molecules form single-layered "blackberry"-type structures mediated by electrostatic interaction, showing the property of macroions. Consequently, a small, accurately controllable design on the molecular structure leads to completely different self-assembled structures, achieved by tuning the relative strengths of different intermolecular forces. This might enlighten us to find various pathways for rationally designing complex self-assembled structures in the future.

■ ASSOCIATED CONTENT

Supporting Information

The Supporting Information is available free of charge on the ACS Publications website at DOI: 10.1021/acs.macromol.7b00963.

^{1}H NMR, ^{13}C NMR, MS, and GPC results for the products or intermediates and light scattering results with different water content or at different concentrations or angles (PDF)

■ AUTHOR INFORMATION

Corresponding Authors

*E-mail: tliu@uakron.edu (T.L.).

*E-mail: scheng@uakron.edu (S.Z.D.C.).

ORCID

Wei Zhang: 0000-0002-9321-6411

Yuchu Liu: 0000-0001-9780-8724

Tianbo Liu: 0000-0002-8181-1790

Stephen Z. D. Cheng: 0000-0003-1448-0546

Author Contributions

W.Z. and Y.C. contributed equally to this work.

DOI: 10.1021/acs.macromol.7b00963
Macromolecules XXXX, XXX, XXX−XXX

Notes

The authors declare no competing financial interest.

■ ACKNOWLEDGMENTS

T.L. acknowledges support from the NSF (CHE1607138) and the University of Akron. S.Z.D.C. acknowledges support from NSF (DMR-1408872). We thank Prof. Chrys Wesdemiotis and Miss Jialin Mao for the help of MALDI-TOF measurements.

■ REFERENCES

(1) Brunsveld, L.; Folmer, B. J. B.; Meijer, E. W.; Sijbesma, R. P. Supramolecular Polymers. *Chem. Rev.* **2001**, *101*, 4071−4098.

(2) Liu, T.; Diemann, E.; Li, H.; Dress, A. W. M.; Muller, A. Self-assembly in aqueous solution of wheel-shaped Mo154 oxide clusters into vesicles. *Nature* **2003**, *426*, 59−62.

(3) Kewalramani, S.; Guerrero-García, G. I.; Moreau, L. M.; Zwanikken, J. W.; Mirkin, C. A.; Olvera de la Cruz, M.; Bedzyk, M. J. Electrolyte-Mediated Assembly of Charged Nanoparticles. *ACS Cent. Sci.* **2016**, *2*, 219−224.

(4) Hunt, J. N.; Feldman, K. E.; Lynd, N. A.; Deek, J.; Campos, L. M.; Spruell, J. M.; Hernandez, B. M.; Kramer, E. J.; Hawker, C. J. Tunable, High Modulus Hydrogels Driven by Ionic Coacervation. *Adv. Mater.* **2011**, *23*, 2327−2331.

(5) Raffa, P.; Wever, D. A. Z.; Picchioni, F.; Broekhuis, A. A. Polymeric Surfactants: Synthesis, Properties, and Links to Applications. *Chem. Rev.* **2015**, *115*, 8504−8563.

(6) Cook, T. R.; Zheng, Y.-R.; Stang, P. J. Metal−Organic Frameworks and Self-Assembled Supramolecular Coordination Complexes: Comparing and Contrasting the Design, Synthesis, and Functionality of Metal−Organic Materials. *Chem. Rev.* **2013**, *113*, 734−777.

(7) Yoneya, M.; Tsuzuki, S.; Yamaguchi, T.; Sato, S.; Fujita, M. Coordination-Directed Self-Assembly of M12L24 Nanocage: Effects of Kinetic Trapping on the Assembly Process. *ACS Nano* **2014**, *8*, 1290−1296.

(8) Babu, S. S.; Praveen, V. K.; Ajayaghosh, A. Functional π-Gelators and Their Applications. *Chem. Rev.* **2014**, *114*, 1973−2129.

(9) Chen, Z.; Cui, H.; Hales, K.; Li, Z.; Qi, K.; Pochan, D. J.; Wooley, K. L. Unique Toroidal Morphology from Composition and Sequence Control of Triblock Copolymers. *J. Am. Chem. Soc.* **2005**, *127*, 8592−8593.

(10) Cui, H.; Chen, Z.; Zhong, S.; Wooley, K. L.; Pochan, D. J. Block Copolymer Assembly via Kinetic Control. *Science* **2007**, *317*, 647−650.

(11) Lodge, T. P.; Hillmyer, M. A.; Zhou, Z.; Talmon, Y. Access to the Superstrong Segregation Regime with Nonionic ABC Copolymers. *Macromolecules* **2004**, *37*, 6680−6682.

(12) Moughton, A. O.; Hillmyer, M. A.; Lodge, T. P. Multicompartment Block Polymer Micelles. *Macromolecules* **2012**, *45*, 2−19.

(13) Zhao, W.; Chen, D.; Hu, Y.; Grason, G. M.; Russell, T. P. ABC Triblock Copolymer Vesicles with Mesh-Like Morphology. *ACS Nano* **2011**, *5*, 486−492.

(14) Ahmad Nor, Y.; Niu, Y.; Karmakar, S.; Zhou, L.; Xu, C.; Zhang, J.; Zhang, H.; Yu, M.; Mahony, D.; Mitter, N.; Cooper, M. A.; Yu, C. Shaping Nanoparticles with Hydrophilic Compositions and Hydrophobic Properties as Nanocarriers for Antibiotic Delivery. *ACS Cent. Sci.* **2015**, *1*, 328−334.

(15) Sun, J.; Jiang, X.; Lund, R.; Downing, K. H.; Balsara, N. P.; Zuckermann, R. N. Self-assembly of crystalline nanotubes from monodisperse amphiphilic diblock copolypeptoid tiles. *Proc. Natl. Acad. Sci. U. S. A.* **2016**, *113*, 3954−3959.

(16) Matyjaszewski, K. Architecturally Complex Polymers with Controlled Heterogeneity. *Science* **2011**, *333*, 1104−1105.

(17) Cho, A.; La, Y.; Shin, T. J.; Park, C.; Kim, K. T. Structural Requirements of Block Copolymers for Self-Assembly into Inverse Bicontinuous Cubic Mesophases in Solution. *Macromolecules* **2016**, *49*, 4510−4519.

(18) Lu, J.; Bates, F. S.; Lodge, T. P. Remarkable Effect of Molecular Architecture on Chain Exchange in Triblock Copolymer Micelles. *Macromolecules* **2015**, *48*, 2667−2676.

(19) Rosen, B. M.; Wilson, C. J.; Wilson, D. A.; Peterca, M.; Imam, M. R.; Percec, V. Dendron-Mediated Self-Assembly, Disassembly, and Self-Organization of Complex Systems. *Chem. Rev.* **2009**, *109*, 6275−6540.

(20) Xiao, Q.; Wang, Z.; Williams, D.; Leowanawat, P.; Peterca, M.; Sherman, S. E.; Zhang, S.; Hammer, D. A.; Heiney, P. A.; King, S. R.; Markovitz, D. M.; André, S.; Gabius, H.-J.; Klein, M. L.; Percec, V. Why Do Membranes of Some Unhealthy Cells Adopt a Cubic Architecture? *ACS Cent. Sci.* **2016**, *2*, 943−953.

(21) Hosono, N.; Gochomori, M.; Matsuda, R.; Sato, H.; Kitagawa, S. Metal−Organic Polyhedral Core as a Versatile Scaffold for Divergent and Convergent Star Polymer Synthesis. *J. Am. Chem. Soc.* **2016**, *138*, 6525−6531.

(22) Zhang, W.; Fang, B.; Walther, A.; Müller, A. H. E. Synthesis via RAFT Polymerization of Tadpole-Shaped Organic/Inorganic Hybrid Poly(acrylic acid) Containing Polyhedral Oligomeric Silsesquioxane (POSS) and Their Self-assembly in Water. *Macromolecules* **2009**, *42*, 2563−2569.

(23) Shi, W.; Tateishi, Y.; Li, W.; Hawker, C. J.; Fredrickson, G. H.; Kramer, E. J. Producing Small Domain Features Using Miktoarm Block Copolymers with Large Interaction Parameters. *ACS Macro Lett.* **2015**, *4*, 1287−1292.

(24) Li, W.; Thanneeru, S.; Kanyo, I.; Liu, B.; He, J. Amphiphilic Hybrid Nano Building Blocks with Surfactant-Mimicking Structures. *ACS Macro Lett.* **2015**, *4*, 736−740.

(25) Zeng, H.; Johnson, M. E.; Oldenhuis, N. J.; Tiambeng, T. N.; Guan, Z. Structure-Based Design of Dendritic Peptide Bolaamphiphiles for siRNA Delivery. *ACS Cent. Sci.* **2015**, *1*, 303−312.

(26) Tamesue, S.; Ohtani, M.; Yamada, K.; Ishida, Y.; Spruell, J. M.; Lynd, N. A.; Hawker, C. J.; Aida, T. Linear versus Dendritic Molecular Binders for Hydrogel Network Formation with Clay Nanosheets: Studies with ABA Triblock Copolyethers Carrying Guanidinium Ion Pendants. *J. Am. Chem. Soc.* **2013**, *135*, 15650−15655.

(27) Jin, H.; Xu, Y.; Shen, Z.; Zou, D.; Wang, D.; Zhang, W.; Fan, X.; Zhou, Q. Jacketed Polymers with Dendritic Carbazole Side Groups and Their Applications in Blue Light-Emitting Diodes. *Macromolecules* **2010**, *43*, 8468−8478.

(28) Lu, Y.; Debnath, D.; Weiss, R. A.; Pugh, C. Synthesis and crosslinking of hyperbranched poly(n-nonyl acrylate) to form organogels. *J. Polym. Sci., Part A: Polym. Chem.* **2015**, *53*, 2399−2410.

(29) Zhang, W.-B.; Yu, X.; Wang, C.-L.; Sun, H.-J.; Hsieh, I. F.; Li, Y.; Dong, X.-H.; Yue, K.; Van Horn, R.; Cheng, S. Z. D. Molecular Nanoparticles Are Unique Elements for Macromolecular Science: From "Nanoatoms" to Giant Molecules. *Macromolecules* **2014**, *47*, 1221−1239.

(30) Yu, X.; Zhong, S.; Li, X.; Tu, Y.; Yang, S.; Van Horn, R. M.; Ni, C.; Pochan, D. J.; Quirk, R. P.; Wesdemiotis, C.; Zhang, W.-B.; Cheng, S. Z. D. A Giant Surfactant of Polystyrene−(Carboxylic Acid-Functionalized Polyhedral Oligomeric Silsesquioxane) Amphiphile with Highly Stretched Polystyrene Tails in Micellar Assemblies. *J. Am. Chem. Soc.* **2010**, *132*, 16741−16744.

(31) Yu, X.; Yue, K.; Hsieh, I.-F.; Li, Y.; Dong, X.-H.; Liu, C.; Xin, Y.; Wang, H.-F.; Shi, A.-C.; Newkome, G. R.; Ho, R.-M.; Chen, E.-Q.; Zhang, W.-B.; Cheng, S. Z. D. Giant surfactants provide a versatile platform for sub-10-nm nanostructure engineering. *Proc. Natl. Acad. Sci. U. S. A.* **2013**, *110*, 10078−10083.

(32) Zhang, W.; Huang, M.; Su, H.; Zhang, S.; Yue, K.; Dong, X.-H.; Li, X.; Liu, H.; Zhang, S.; Wesdemiotis, C.; Lotz, B.; Zhang, W.-B.; Li, Y.; Cheng, S. Z. D. Toward Controlled Hierarchical Heterogeneities in Giant Molecules with Precisely Arranged Nano Building Blocks. *ACS Cent. Sci.* **2016**, *2*, 48−54.

(33) Li, D.; Niu, Y.; Yang, Y.; Wang, X.; Yang, F.; Shen, H.; Wu, D. Synthesis and self-assembly behavior of POSS-embedded hyperbranched polymers. *Chem. Commun.* **2015**, *51*, 8296−8299.

(34) Liu, H.; Luo, J.; Shan, W.; Guo, D.; Wang, J.; Hsu, C.-H.; Huang, M.; Zhang, W.; Lotz, B.; Zhang, W.-B.; Liu, T.; Yue, K.;

DOI: 10.1021/acs.macromol.7b00963
Macromolecules XXXX, XXX, XXX−XXX

Cheng, S. Z. D. Manipulation of Self-Assembled Nanostructure Dimensions in Molecular Janus Particles. *ACS Nano* **2016**, *10*, 6585−6596.

(35) Yu, X.; Zhang, W.-B.; Yue, K.; Li, X.; Liu, H.; Xin, Y.; Wang, C.-L.; Wesdemiotis, C.; Cheng, S. Z. D. Giant Molecular Shape Amphiphiles Based on Polystyrene−Hydrophilic [60]Fullerene Conjugates: Click Synthesis, Solution Self-Assembly, and Phase Behavior. *J. Am. Chem. Soc.* **2012**, *134*, 7780−7787.

(36) Lam, C. N.; Olsen, B. D. Phase transitions in concentrated solution self-assembly of globular protein-polymer block copolymers. *Soft Matter* **2013**, *9*, 2393−2402.

(37) Chu, Y.; Zhang, W.; Lu, X.; Mu, G.; Zhang, B.; Li, Y.; Cheng, S. Z. D.; Liu, T. Rational controlled morphological transitions in the self-assembled multi-headed giant surfactants in solution. *Chem. Commun.* **2016**, *52*, 8687−8690.

(38) Li, Y.; Dong, X.-H.; Guo, K.; Wang, Z.; Chen, Z.; Wesdemiotis, C.; Quirk, R. P.; Zhang, W.-B.; Cheng, S. Z. D. Synthesis of Shape Amphiphiles Based on POSS Tethered with Two Symmetric/Asymmetric Polymer Tails via Sequential "Grafting-from" and Thiol−Ene "Click" Chemistry. *ACS Macro Lett.* **2012**, *1*, 834−839.

(39) Li, D.; Song, J.; Yin, P.; Simotwo, S.; Bassler, A. J.; Aung, Y.; Roberts, J. E.; Hardcastle, K. I.; Hill, C. L.; Liu, T. Inorganic−Organic Hybrid Vesicles with Counterion- and pH-Controlled Fluorescent Properties. *J. Am. Chem. Soc.* **2011**, *133*, 14010−14016.

(40) Chu, Y.; Saad, A.; Yin, P.; Wu, J.; Oms, O.; Dolbecq, A.; Mialane, P.; Liu, T. Light- and Solvent-Controlled Self-Assembly Behavior of Spiropyran−Polyoxometalate−Alkyl Hybrid Molecules. *Chem. - Eur. J.* **2016**, *22*, 11756−11762.

(41) Cobo, I.; Li, M.; Sumerlin, B. S.; Perrier, S. Smart hybrid materials by conjugation of responsive polymers to biomacromolecules. *Nat. Mater.* **2014**, *14*, 143−159.

(42) Gao, Y.; Szymanowski, J. E. S.; Sun, X.; Burns, P. C.; Liu, T. Thermal Responsive Ion Selectivity of Uranyl Peroxide Nanocages: An Inorganic Mimic of K+ Ion Channels. *Angew. Chem., Int. Ed.* **2016**, *55*, 6887−6891.

(43) Wu, K.; Huang, M.; Yue, K.; Liu, C.; Lin, Z.; Liu, H.; Zhang, W.; Hsu, C.-H.; Shi, A.-C.; Zhang, W.-B.; Cheng, S. Z. D. Asymmetric Giant "Bolaform-like" Surfactants: Precise Synthesis, Phase Diagram, and Crystallization-Induced Phase Separation. *Macromolecules* **2014**, *47*, 4622−4633.

(44) Yue, K.; Huang, M.; Marson, R. L.; He, J.; Huang, J.; Zhou, Z.; Wang, J.; Liu, C.; Yan, X.; Wu, K.; Guo, Z.; Liu, H.; Zhang, W.; Ni, P.; Wesdemiotis, C.; Zhang, W.-B.; Glotzer, S. C.; Cheng, S. Z. D. Geometry induced sequence of nanoscale Frank−Kasper and quasicrystal mesophases in giant surfactants. *Proc. Natl. Acad. Sci. U. S. A.* **2016**, *113*, 14195−14200.

(45) Yin, P.; Li, D.; Liu, T. Solution behaviors and self-assembly of polyoxometalates as models of macroions and amphiphilic polyoxometalate-organic hybrids as novel surfactants. *Chem. Soc. Rev.* **2012**, *41*, 7368−7383.

(46) Yin, P.; Zhang, Z.-M.; Lv, H.; Li, T.; Haso, F.; Hu, L.; Zhang, B.; Bacsa, J.; Wei, Y.; Gao, Y.; Hou, Y.; Li, Y.-G.; Hill, C. L.; Wang, E.-B.; Liu, T. Chiral recognition and selection during the self-assembly process of protein-mimic macroanions. *Nat. Commun.* **2015**, *6*, 6475.

(47) Zhou, J.; Yin, P.; Hu, L.; Haso, F.; Liu, T. Self-Assembly of Subnanometer-Scaled Polyhedral Oligomeric Silsesquioxane (POSS) Macroions in Dilute Solution. *Eur. J. Inorg. Chem.* **2014**, *2014*, 4593−4599.

(48) Liu, T. Hydrophilic Macroionic Solutions: What Happens When Soluble Ions Reach the Size of Nanometer Scale? *Langmuir* **2010**, *26*, 9202−9213.

(49) Liu, T. An Unusually Slow Self-Assembly of Inorganic Ions in Dilute Aqueous Solution. *J. Am. Chem. Soc.* **2003**, *125*, 312−313.

(50) Zhang, B.; Pradeep, C. P.; Cronin, L.; Liu, T. Self-assembly of triangular polyoxometalate-organic hybrid macroions in mixed solvents. *Chem. Commun.* **2015**, *51*, 8630−8633.

(51) Yin, P.; Lin, Z.; Wu, J.; Hsu, C.-H.; Chen, X.; Zhou, J.; Lu, P.; Eghtesadi, S. A.; Yu, X.; Cheng, S. Z. D.; Liu, T. Charge-Regulated Spontaneous, Reversible Self-Assembly of the Carboxylic Acid-Functionalized Hydrophilic Fullerene Macroanions in Dilute Solution. *Macromolecules* **2015**, *48*, 725−731.

(52) Li, Y.; Guo, K.; Su, H.; Li, X.; Feng, X.; Wang, Z.; Zhang, W.; Zhu, S.; Wesdemiotis, C.; Cheng, S. Z. D.; Zhang, W.-B. Tuning "thiol-ene" reactions toward controlled symmetry breaking in polyhedral oligomeric silsesquioxanes. *Chem. Sci.* **2014**, *5*, 1046−1053.

(53) Liu, Z.; Liu, T.; Tsige, M. Elucidating the Origin of the Attractive Force among Hydrophilic Macroions. *Sci. Rep.* **2016**, *6*, 26595.

(54) Verhoeff, A. A.; Kistler, M. L.; Bhatt, A.; Pigga, J.; Groenewold, J.; Klokkenburg, M.; Veen, S.; Roy, S.; Liu, T.; Kegel, W. K. Charge Regulation as a Stabilization Mechanism for Shell-Like Assemblies of Polyoxometalates. *Phys. Rev. Lett.* **2007**, *99*, 066104.

DOI: 10.1021/acs.macromol.7b00963
Macromolecules XXXX, XXX, XXX−XXX